23rd ABCM International Congress of Mechanical Engineering
December 6-11, 2015, Rio de Janeiro, RJ, Brazil

AERODYNAMIC LOADS FOR AEROELASTIC ANALYSES USING HIGH-FIDELITY COMPUTATIONAL FLUID DYNAMICS

Rafael N. Ihi
Instituto Tecnológico de Aeronáutica, DCTA/ITA, São José dos Campos, SP, Brazil
rafael.ihi@hotmail.com

João Luiz F. Azevedo
Instituto de Aeronáutica e Espaço, DCTA/IAE/ALA, São José dos Campos, SP, Brazil
joaoluiz.azevedo@gmail.com

Abstract. *The present work focus on the use of a more realistic computational fluid dynamics (CFD) formulation in the construction of the aerodynamic operator for aeroelastic stability analyses. The emphasis in the work is in the calculation of the unsteady aerodynamic loads and on the effects of the inclusion of the viscous terms in the aerodynamic transfer functions. The aeroelastic formulation for a typical section airfoil is presented in order to demonstrate how such unsteady loads influence the system dynamics. The flows of interest are assumed to be adequately modeled by the 2-D Euler equations or the 2-D Reynolds-averaged Navier-Stokes (RANS) equations with appropriate turbulence closures. The dynamic system is represented by the NACA 0012 airfoil typical section with two degrees of freedom, plunge and pitch. The purely aerodynamic test cases considered for the airfoil, in the transonic regime, include steady and harmonic prescribed motions. Indicial aerodynamic responses of the airfoil, with the current flow solver formulation, are compared to purely inviscid calculations.*

Keywords: *Unsteady aerodynamics, CFD, Typical section.*

1. INTRODUCTION

The fluid-structure interaction problem plays an important role in many industrial applications of engineering systems. In aeronautics, for instance, it is a crucial item to be considered, since this interaction generates vibrations, which in turn can cause structural fatigue and, even, aeroelastic phenomena, such as buffeting, aileron reversal, or flutter, for example. These problems are often very complex, involving the coupling effects of the fluid flow interacting with a moving elastic structure. Recent advances in computational performance, along with the computational fluid dynamics (CFD) techniques, made the numerical approach to this problem feasible in an industrial context. Nevertheless, there is still considerable room for improvement in the tools available and in the computational costs for such analyses in this research area.

The present work is focused on the numerical investigation of the fluid-structure interaction for transonic flows over the NACA 0012 airfoil, and the validation of a CFD tool developed for such aeroelastic applications through the comparison of aerodynamic coefficients. The Reynolds number (Re) considered for the simulations is $Re = 12\times10^6$. Simulations are based on the 2-D Euler equations or the 2-D Reynolds-averaged Navier-Stokes (RANS) equations, and no deformation of the airfoil is considered. A typical airfoil section model is used, in which the torsion and flexure of a real wing configuration are represented by the pitch and plunge degrees of freedom, respectively. The unsteady flows deal with prescribed step and sinusoidal motions of the airfoil. In the former case of motion, the lift and moment coefficients are compared with the inviscid results of Marques and Azevedo (2008a) in order to validate the implementation of the viscous terms, recently accomplished. For harmonic motions, the aerodynamic hysteresis is investigated as a form of demonstrating the capability of the solver to run unsteady simulations.

2. GENERAL FORMULATION

2.1 Aeroelasticity

The aeroelastic structural model is represented by the typical section (Bisplinghoff *et al.*, 1995; Weisshaar, 2010). This system consists of a rigid airfoil, mounted on torsional and cross-flow springs, as shown in Fig. 1. The airfoil has two degrees of freedom, plunge and pitch, and it is able move under the effect of the aerodynamic, inertial and elastic loadings. A state space representation of the typical section system can be written as

$$\left[\tilde{M}\right]\{\dot{\chi}(t^*)\} + \left[\tilde{K}\right]\{\chi(t^*)\} = \{\tilde{Q}_a(t^*)\}\,, \qquad (1)$$

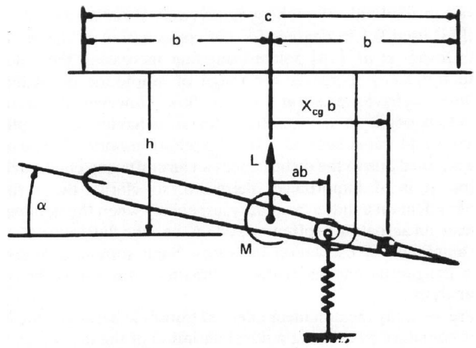

Figure 1. Typical section airfoil.

where $\{\chi(t^*)\}$ is the system state vector,

$$\{\chi_1(t^*)\} = \{\eta(t^*)\} \,, \tag{2}$$

$$\{\chi_2(t^*)\} = \{\dot{\eta}(t^*)\} = \{\dot{\chi_1}(t^*)\} \,, \tag{3}$$

$$\{\chi(t^*)\} = \left\{ \begin{array}{c} \{\chi_2(t^*)\} \\ \{\chi_1(t^*)\} \end{array} \right\} . \tag{4}$$

The dimensionless mass and stiffness matrices, $[\tilde{M}]$ and $[\tilde{K}]$, are defined, respectively, as

$$[\tilde{M}] = \left[\begin{array}{cc} [M^*] & [0_{2\times2}] \\ [0_{2\times2}] & [I_{2\times2}] \end{array} \right] \,, \; [\tilde{K}] = \left[\begin{array}{cc} [0_{2\times2}] & [K^*] \\ [-I_{2\times2}] & [0_{2\times2}] \end{array} \right] \,, \tag{5}$$

where the $[M^*]$ and $[K^*]$ matrices are defined in Marques and Azevedo (2008b), and the forcing term is given by

$$\{\tilde{Q_a}(t^*)\} = \left\{ \begin{array}{c} \{{Q_a}^*(t^*)\} \\ \{0_{2\times1}\} \end{array} \right\} \,, \tag{6}$$

here, $\{{Q_a}^*(t^*)\}$ is the appropriately normalized vector of the generalized modal aerodynamic forces. Applying the Laplace transform to Eq. 1, one obtains

$$s^* \left[\tilde{M}\right] \{X(s^*)\} + \left[\tilde{K}\right] \{X(s^*)\} = \{\tilde{Q_a}(s^*)\} \,, \tag{7}$$

where

$$s^* = \frac{s}{\omega_r} \,. \tag{8}$$

The general state space representation of the typical section aeroelastic system is described by the following expression

$$\{\dot{\mathcal{Z}}(t^*)\} = [D] \{\mathcal{Z}(t^*)\} \,, \tag{9}$$

where the stability matrix, $[D]$, is defined in Marques and Azevedo (2008b) and $\{\mathcal{Z}(t^*)\}$ is the new state vector that results from the addition of the aerodynamic state variables. This vector is written as

$$\{\mathcal{Z}(t^*)\} = \left\{ \begin{array}{c} \{\dot{\eta}(t^*)\} \\ \{\eta(t^*)\} \\ \{\eta_a(t^*)\}_1 \\ \vdots \\ \{\eta_a(t^*)\}_{n_a} \end{array} \right\} \,, \tag{10}$$

and

$$\{\eta_a(t^*)\}_n = \int_0^{t^*} \{\eta(\tau)\} e^{[-V^* \beta_n (t^* - \tau)]} d\tau \,, \tag{11}$$

where the β_n variables introduce the aerodynamic lags with respect to the structural modes and n_a is the number of added aerodynamic state variables. Furthermore, the generalized aerodynamic force vector is, then, written in terms of the new aerodynamic state variables as

$$\{Q_a(t^*)\} = \frac{(V^*)^2}{\pi\mu_r}\left([A_0]\{\eta(t^*)\} + \frac{1}{V^*}[A_1]\{\dot{\eta}(t^*)\} + \right.$$
$$\left. + \frac{1}{(V^*)^2}[A_2]\{\ddot{\eta}(t^*)\} + \sum_{n=1}^{n_\beta}\left[A_{(n+2)}\right]\{\eta_a(t^*)\}_n\right) . \tag{12}$$

Here, the $[A_n]$ matrices are the approximating coefficient matrices. Furthermore,

$$[{Q_a}^*(t^*)] = \frac{1}{\omega_r^2}\left[Q_a(t^*)\right] . \tag{13}$$

The aeroelastic stability analysis can be reduced to the classical eigenvalue problem as

$$([D] - s^*\left[I_{n\times n}\right])\left\{\mathcal{Z}\left(s^*\right)\right\} = \{0_{n\times 1}\} . \tag{14}$$

The objective here is to evaluate the behavior of this system as a function of the characteristic speed, V^*, which is defined as

$$V^* = \frac{U_\infty}{b\omega_r} , \tag{15}$$

where b is the airfoil half chord and ω_r is the circular reference frequency.

2.2 Aerodynamics

The CFD tool used in this work is based on the 2-D RANS equations, which represent a two dimensional flow of a compressible viscous fluid through a continuous medium in the transient regime. In a finite volume approach, these equations can be written in Cartesian coordinates as

$$\frac{\partial}{\partial t}\int_{V_i} Q dxdy + \oint_{S_i}(Edy - Fdx) = 0 . \tag{16}$$

In Eq. 16, V represents the control volume or the area, and S is the length of the edges of the cells. Q is the vector of conserved properties, and E and F are the flux vectors in the x and y directions, respectively. These variables are written

$$Q = [\ \rho \quad \rho u \quad \rho v \quad e\ ]^T , \qquad E = E_e - E_v, \qquad F = F_e - F_v . \tag{17}$$

Here, E_e and F_e represent the inviscid fluxes, or Euler fluxes, whereas E_v and F_v represent the viscous terms (Azevedo *et al.*, 2013). In addition, the set of Euler equations are obtained from the Navier-Stokes equations by neglecting all viscous stresses and heat conduction terms.

In the present work, turbulence closure is achieved with the Spalart-Allmaras (SA) turbulence model (Spalart and Allmaras, 1994). It is implemented in the solver in accordance to the formulation presented in Spalart and Allmaras (1994). The model is concurrently integrated with the 2-D RANS equations in a loosely coupled approach (Bigarella and Azevedo, 2007).

2.3 Spatial Discretization

The numerical scheme adopted in this work is a cell centered finite volume method (Azevedo *et al.*, 2013). Here, for each control volume face, flux information of flow field variables are computed from i-th and n_b-th control volumes which share a k-th face. The flux computation is, then, accordingly distributed back to the i-th and n_b-th control volumes. Moreover, all variables or parameters necessary at face are computed by a simple average procedure. Further details can be found in Marques and Azevedo (2008a); Azevedo *et al.* (2013); Mavriplis (1990).

2.4 Time Discretization

For calculations without dual time stepping (DTS), an explicit, 2nd-order, 5-stage Runge-Kutta scheme (Marques and Azevedo, 2008a) is used to integrate the RANS equations in time, while a 1st-order implicit Euler method (Bigarella and Azevedo, 2007) is used to time advance the turbulence model equation. For applications in which a dual time stepping method is required, a 2nd-order implicit backward Euler scheme (Lomax *et al.*, 2001) is used to discretize the physical time derivatives for the RANS equations, whereas the same explicit 5-stage Runge-Kutta scheme (Marques and Azevedo, 2008a) is used for time stepping in pseudo time. As before, the turbulence modeling equation is time-marched with the 1st-order implicit Euler method (Bigarella and Azevedo, 2007). This equation is not subjected to dual time stepping, since the flow and the turbulence model equations are time marched in a loosely coupled fashion. The approach is able to increase the stability range of the method, allowing larger time steps which are, therefore, only bound by the physical frequencies one wishes to resolve in the unsteady simulations.

3. Mesh Generation

The computational mesh generation is a process of extreme importance and plays a crucial role in the overall CFD solution. The quality and accuracy of a CFD outcome is very dependent on the mesh properties (Hirsch, 1988). Each mesh should be specifically designed in accordance to the flow condition, intended to be simulated, and the physical phenomena of interest, which can be relevant to the solution. The mesh used in the present work is generated with the ICEM CFD© commercial grid generator. Such tool is capable of creating sophisticated meshes, with very good grid quality control, as the ones required for the current work. The NACA 0012 airfoil grid designed for the turbulent high-Reynolds number flow is composed of $69,324$ quadrilateral cells, as illustrated in Fig. 2. This figure shows two views of the unstructured mesh around the airfoil. Moreover, the farfield distance is set to 50 chord lengths. The non-dimensional distance in the current

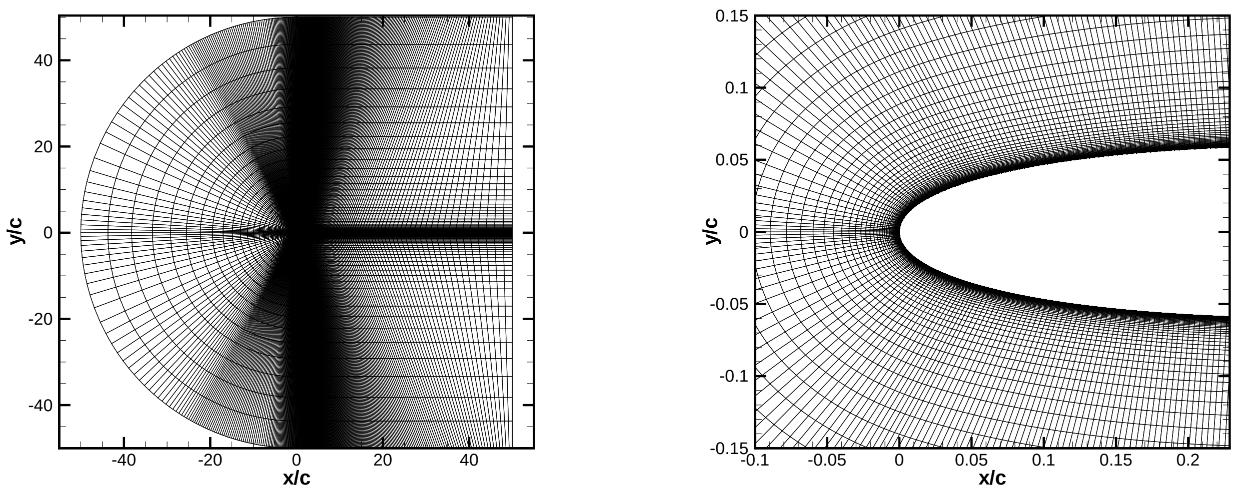

(a) Complete mesh, with 69950 nodes and 69324 volumes.

(b) Mesh view closer to the airfoil leading edge.

Figure 2. RANS solver mesh around the NACA 0012 airfoil.

cell-centered finite volume context, usually adopted for the Spalart-Allmaras turbulence closure, is $y^+ \leq 1$ (Bigarella, 2007). Therefore, this restriction is respected over the entire wall boundary in order to avoid a less than adequate behavior of the turbulence closure used. This dimensionless distance to the wall of the first point off the wall is defined as

$$y^+ = y_1 \frac{u_\tau}{\nu} \, , \tag{18}$$

where y_1 is the distance from the nearest wall node to the adjacent wall and u_τ is the friction velocity, which is defined as

$$u_\tau = \sqrt{\frac{\tau_w}{\rho}} \quad , \qquad \tau_w = \mu \left(\frac{\partial u}{\partial y} \right)_{wall} \, . \tag{19}$$

Here, τ_w represents the wall shear stress for a 2-D flow.

4. RESULTS

4.1 Validation of the Unsteady Solver

The investigation of aerodynamic hysteresis in unsteady transonic flows is very important as a form of characterizing the behavior of the flow simulation code under controlled unsteady conditions and for very smooth motions. Moreover, such investigation allows a verification of the mesh movement procedures implemented in the solver. This aerodynamic hysteresis phenomenon can be used to validate the unsteady results against data available in the literature, as well as it can be used to estimate the effect of the phase lag between the motion and the aerodynamic response. In the present work, the oscillatory motion of the harmonically pitching airfoil is obtained by specifying the angle of attack variation.

The NACA 0012 airfoil is forced by a harmonic oscillation in the pitch degree of freedom about the quarter chord point. The simulations are performed using an Euler formulation. The unsteady lift and moment coefficients for the pitching NACA 0012 airfoil at $M_\infty = 0.755$, $\alpha_0 = 0.016$ deg., $\Delta\alpha = 2.51$ deg., and $k = 0.0814$ are presented in Fig. 3. Here, α_0 is the initial mean flow angle of attack, $\Delta\alpha$ is the pitch oscillation amplitude and k is the reduced frequency. The simulations are performed until the solution reaches a periodic state, which in this case is obtained after four cycles of motion. The dimensionless time step is 0.001. A comparison of the present Euler results is made with the experimental

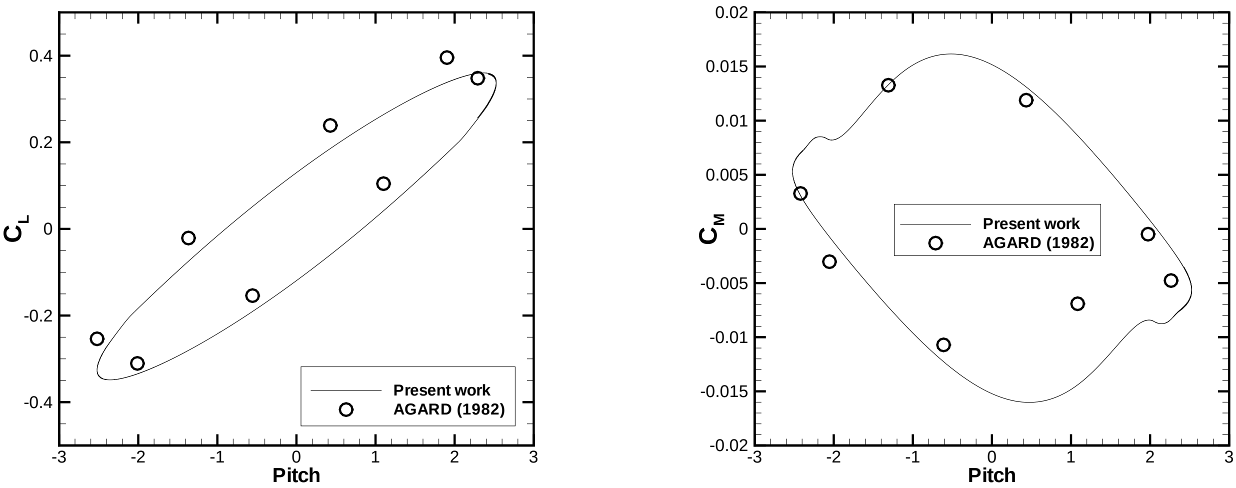

(a) Unsteady lift coefficient response. (b) Unsteady moment coefficient response.

Figure 3. Sinusoidal pitch oscillations of a NACA 0012 airfoil at $M_\infty = 0.755$ and $k = 0.0814$.

data from AGARD (1982), and good agreement is observed. Moreover, it is quite possible that the differences between the numerical and experimental results would be even smaller for viscous runs. The present simulation has also been used as a form of validating the DTS scheme, which is essential for dealing with the stiffness problem created by the very fine meshes required for viscous turbulent calculations. Further details can be found in Ihi and Azevedo (2015), which show that the implemented algorithm is producing the expected results once convergence in the inner iterations has been achieved.

4.2 Indicial Response

As demonstrated in Ballhaus and Goorjian (1978), a series of time-shifted and scaled step functions are equivalent to any continuous function. Hence, the convolution integral of an indicial response with the input time derivative is an approximation of the system response to an arbitrary input. The determination of the indicial response of an aerodynamic system is, therefore, sufficient to know the complete unsteady behavior of that system. These calculations are essential in order to allow the uncoupling of the dynamic equations of motion from the aerodynamic response in aeroelastic problems such as the ones of interest here. In other words, the governing equations for the structural dynamics may be solved separately from the aerodynamic equations.

The investigation on the effects of the inclusion of the viscous terms is performed in comparison with a purely inviscid calculation, obtained in Marques and Azevedo (2008a). Discrete step functions, or DS, are also used to prescribe the airfoil motion, with the intention of measuring the unsteady aerodynamic response. As discussed, the correct calculation of the aerodynamic response for such functions is essential in order to be able to generate aerodynamic transfer functions that would allow performing the stability analysis of the aeroelastic system in the frequency domain.

Freestream conditions considered in these simulations are $M_\infty = 0.8$ and initial steady angle of attack $\alpha_0 = 0$ deg. For the viscous calculations, the freestream Reynolds number considered is $Re = 12 \times 10^6$, based on the airfoil chord. Furthermore, the SA turbulence model is used for turbulence closure in the viscous simulations. The amplitude of the DS input is 0.000001 dimensionless chord units in plunge and 0.0001 deg. in pitch. The time step reported in the inviscid calculations in Marques and Azevedo (2008a) is 0.003 dimensionless time units. A DTS scheme is used to time march the aerodynamic equations, using the same physical time step as the one employed by the reference. The initial 0.15 dimensionless time units of simulation were performed, here, using 1000 inner iterations for each physical time step. Ihi and Azevedo (2015) demonstrates that this number of inner iterations is enough to achieve convergence during the initial stage of the DS input excitation. After this initial period of 0.15 time units, the number of inner iterations decreases to 100. This procedure was necessary to allow the feasibility of the computational cost regarding the turbulent flow simulations.

The lift and moment coefficient responses of a NACA 0012 airfoil subjected to a DS input in plunge and pitch are shown in Figs. 4 and 5, respectively. In these figures, the current results are compared to the ones obtained in Marques and Azevedo (2008a) for a similar study. Figures 4 and 5 indicate that the variation of the aerodynamic responses becomes much smoother after a short period of time from the onset of the DS perturbation. Hence, it is expected that the number of inner iterations required to achieve convergence of the inner iterations would also follow the same tendency of the aerodynamic coefficients time histories, *i.e.*, it would be smaller. Moreover, despite having a fairly pronounced initial

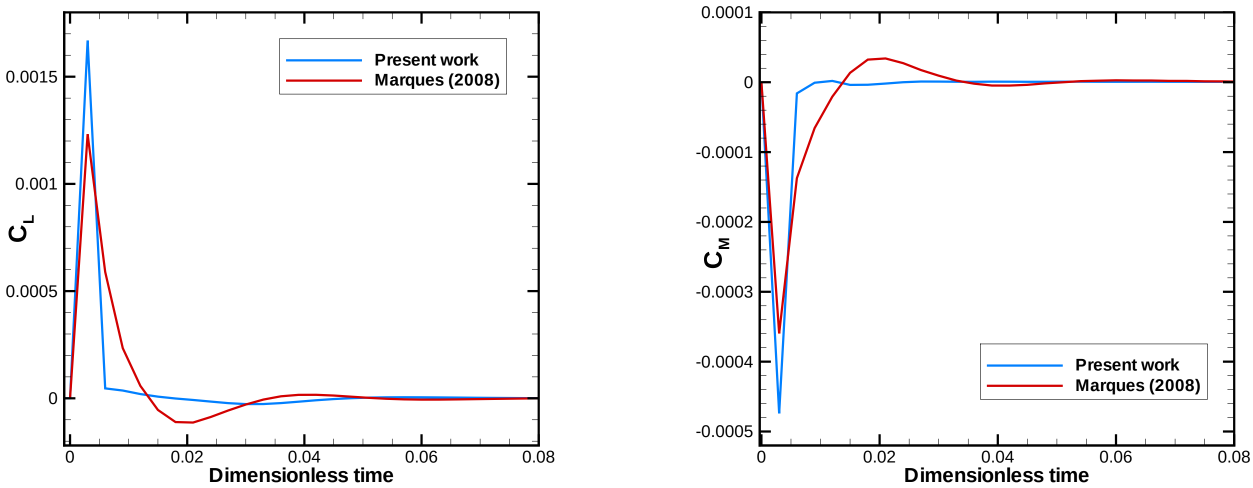

(a) Unsteady lift coefficient response.

(b) Unsteady moment coefficient response.

Figure 4. Aerodynamic response to a discrete step in plunge for a NACA 0012 airfoil at $M_\infty = 0.8$ and $\alpha_0 = 0$ deg.

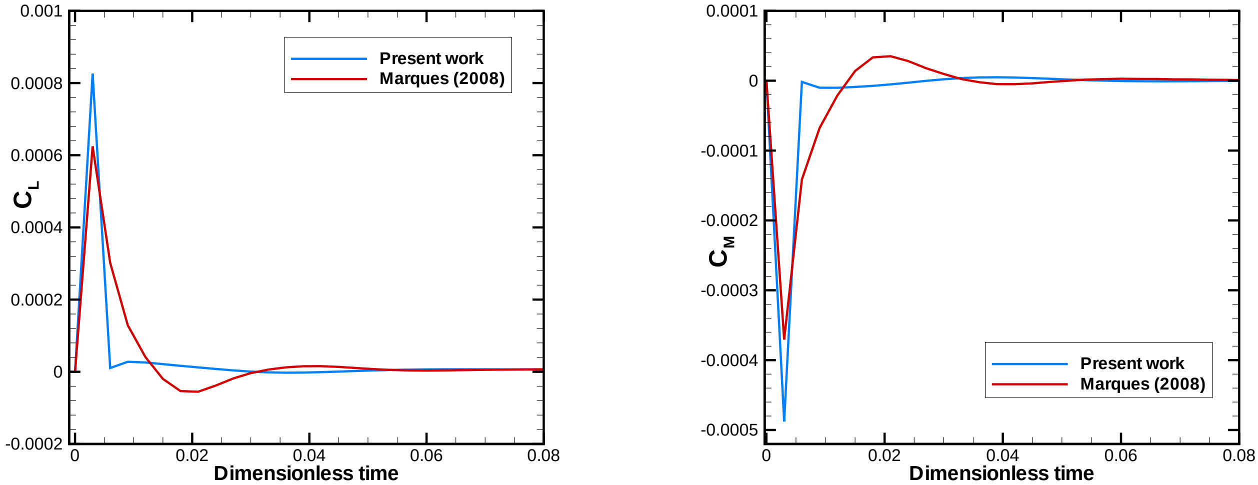

(a) Unsteady lift coefficient response.

(b) Unsteady moment coefficient response.

Figure 5. Aerodynamic response to a discrete step in pitch for a NACA 0012 airfoil at $M_\infty = 0.8$ and $\alpha_0 = 0$ deg.

peak, the viscous response is damped faster than the inviscid one, for all cases, as expected. Additionally, the higher amplitude observed in the initial part of the viscous flow response seems to make sense if one considers the development of a leading edge vortex caused by the unsteady motion. Thus, such vortical structures are responsible for a pressure drop in their vicinity, increasing the lift. Naturally, the lift gain is temporary, once the vortex is quickly convected away from the airfoil, which would explain the damped behavior of the viscous flow response afterwards.

4.3 Aerodynamic Transfer Functions

The major interest, considering the perspective of performing aeroelastic stability analyses, consists in obtaining aerodynamic states from the unsteady aerodynamic responses. The calculation of such aerodynamic states concerns the calculation of aerodynamic transfer functions in the frequency domain and the approximation of such transfer functions using rational polynomials as discussed in Marques and Azevedo (2008a); Azevedo *et al.* (2012). In the case of the present work, the aerodynamic transfer functions are calculated from performing power spectral density calculations of the previous unsteady aerodynamic results, as discussed in detail in Azevedo *et al.* (2012).

The aerodynamic transfer functions are presented in Fig. 6. This figure presents the results in terms of real and imaginary parts of the lift and moment coefficients due to plunge and due to pitch. The present results are compared to those reported in Marques and Azevedo (2008a), which considered an inviscid flow. Clearly, the frequency content of the

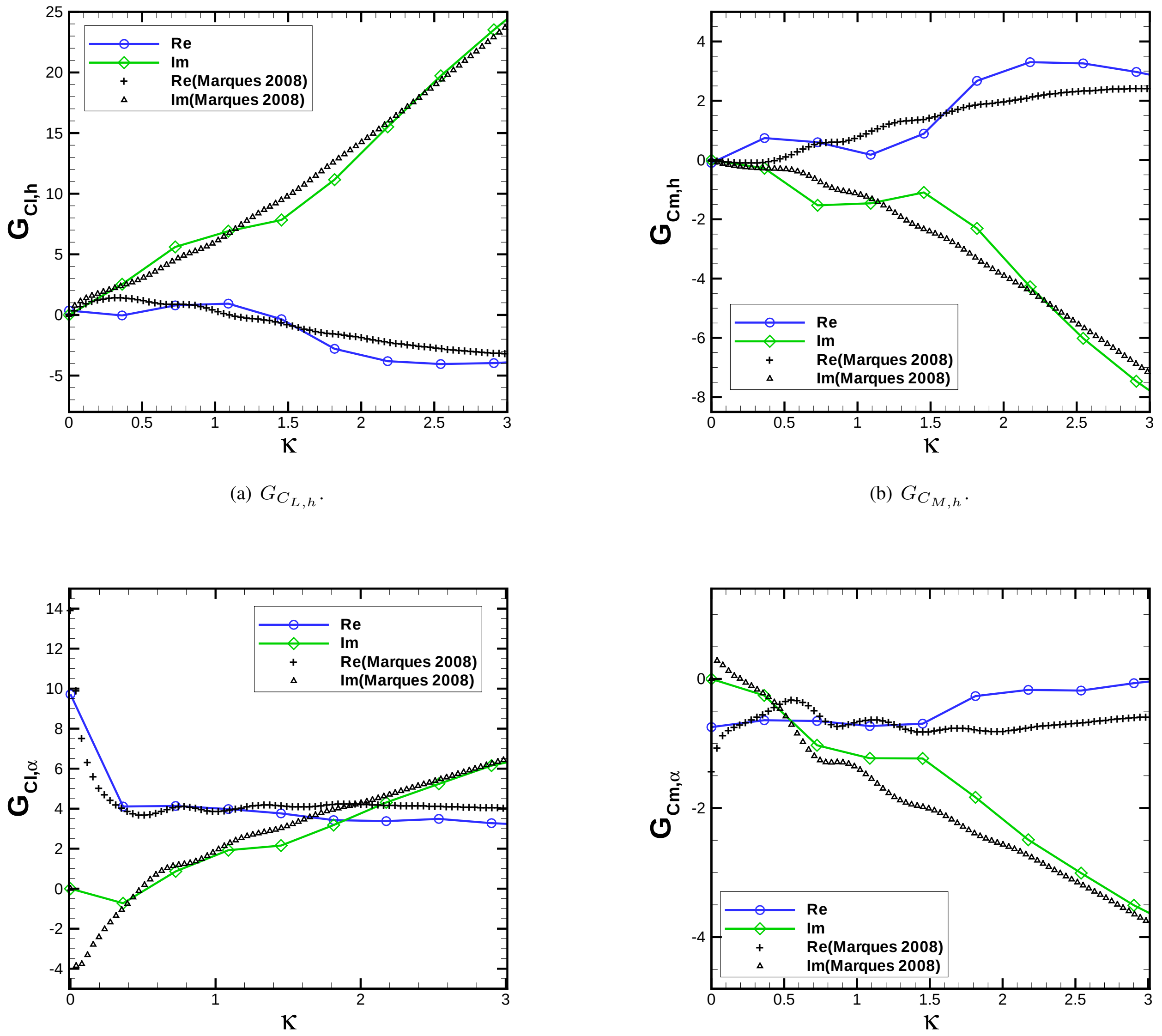

(a) $G_{C_{L,h}}$.

(b) $G_{C_{M,h}}$.

(c) $G_{C_{L,\alpha}}$.

(d) $G_{C_{M,\alpha}}$.

Figure 6. Aerodynamic transfer functions.

current results does not have the same level of resolution as the literature data. The interval of two consecutive points in the frequency domain of the aerodynamic transfer functions is inversely proportional to total integration time of the aerodynamic solution (Azevedo *et al.*, 2012). Thus, it is still premature to evaluate the effects of inclusion of the viscous terms, in the aerodynamic formulation, accurately. In any event, it is also possible to notice from the results that such effects are quite significant, especially in the transfer functions due to pitch. The latter present a very nonlinear behavior, which requires a smaller interval between the data points in order to allow a better polynomial representation of its true behavior. Thus, at this point, it does not make sense to perform a root locus stability analysis of the dynamic system using the obtained transfer functions, because the resolution in the frequency domain is still less than adequate. However, the unsteady simulations are still running at the time of this writing and the authors are hopeful that, at the event, they would have run for long enough that an adequate frequency resolution could be obtained.

5. CONCLUDING REMARKS

A comparative study of the use of inviscid and viscous aerodynamic formulations is performed in order to obtain the aerodynamic loads for aeroelastic analysis using computational fluid dynamics (CFD) techniques in the development of the aerodynamic operator. The work addresses transonic flows over a NACA 0012 airfoil, and it uses the Spalart-

Allmaras turbulence model for turbulence closure when using a viscous formulation, considering the high Reynolds numbers for the flows of interest here. Viscous unsteady aerodynamic calculations here performed are compared to inviscid results previously obtained in the research group. As expected, the viscous formulation provided smoother aerodynamic responses in relation to the inviscid ones. Naturally, such differences impact the aerodynamic transfer functions in the frequency domain. Although it is true that more resolution in the frequency domain is required to allow a fair comparison of the transfer functions, in the aeroelastic system considered here, viscosity appears to play a significant role in the aerodynamic transfer functions. Future work will address the integration of the discrete step response over a larger period of time. This would provide a better resolution of the aerodynamic transfer functions, which in turn, would allow realistic aeroelastic stability analyses.

6. ACKNOWLEDGEMENTS

The authors gratefully acknowledge the partial support for this research provided by Conselho Nacional de Desenvolvimento Científico e Tecnológico, CNPq, under the Research Grants No. 309985/2013-7, No. 400844/2014-1, No. 443839/2014-0 and No. 574004/2008-4. This work is also supported by Fundação Coordenação de Aperfeiçoamento de Pessoal de Nível Superior, CAPES, through a Ph.D. scholarship for the first author. The authors are also indebted to the partial financial support received from Fundação de Amparo à Pesquisa do Estado de São Paulo, FAPESP, under the Research Grants No. 2008/57866-1 and No. 2013/07375-0.

7. REFERENCES

AGARD, 1982. “Compendium of unsteady aerodynamic measurements”. AGARD-R-702.

Azevedo, J.H.A., Azevedo, J.L.F. and Silva, R.G.A., 2012. “Efficient calculation of aerodynamic states for aeroelastic analyses in the frequency domain”. In AIAA Paper No. 2012–1716*, Proceedings of the 53rd AIAA/ASME/ASCE/AHS/ASC Structures, Structural Dynamics and Materials Conference*. Honolulu, Hawaii.

Azevedo, J.L.F., Schiavo, L.A.C.A., Ihi, R.N., Azevedo, J.H.A. and Wolf, W.R., 2013. “Fluid-structure interaction coupling on free moving cylinders in low reynolds number flows”. In *Proceedings of the 11th International Conference on Vibration Problems - ICOVP2013*. Lisbon, Portugal.

Ballhaus, W.F. and Goorjian, P.M., 1978. “Computation of unsteady transonic flows by the indicial method”. *AIAA Journal*, Vol. 16, No. 2, pp. 117–124.

Bigarella, E.D.V., 2007. *Advanced Turbulence Modeling for Complex Aerospace Applications*. Ph.D. thesis, Instituto Tecnológico de Aeronáutica, São José dos Campos, SP, Brasil.

Bigarella, E.D.V. and Azevedo, J.L.F., 2007. “Advanced eddy-viscosity and Reynolds-stress turbulence model simulations of aerospace applications”. *AIAA Journal*, Vol. 45, No. 10, pp. 2369–2390.

Bisplinghoff, R.L., Ashley, H. and Halfman, R.L., 1995. *Aeroelasticity*. Addison-Wesley, Cambridge, MA.

Hirsch, C., 1988. *Numerical Computation of Internal and External Flows, Volume 1, Fundamentals of Numerical Discretization*. John Wiley and Sons, New York.

Ihi, R.N. and Azevedo, J.L.F., 2015. “Comparison of viscous and inviscid unsteady aerodynamic loads for aeroelastic analyses”. In *Proceedings of the 53rd 53rd AIAA Aerospace Sciences Meeting - AIAA2015*. Kissimee, U.S.A.

Lomax, H., Pulliam, T.H. and Zingg, D.W., 2001. *Fundamentals of Computational Fluid Dynamics*. Springer, New York.

Marques, A.N. and Azevedo, J.L.F., 2008a. “Numerical calculation of impulsive and indicial aerodynamic responses using computational aerodynamics techniques”. *Journal of Aircraft*, Vol. 45, No. 4, pp. 1112–1135.

Marques, A.N. and Azevedo, J.L.F., 2008b. “A z-transform discrete-time state-space formulation for aeroelastic stability analysis”. *Journal of Aircraft*, Vol. 45, No. 5, pp. 1564–1578.

Mavriplis, D., 1990. “Accurate multigrid solution of the Euler equations on unstructured and adaptative meshes”. *AIAA Journal*, Vol. 28, No. 2, pp. 213–221.

Spalart, P.R. and Allmaras, S.R., 1994. “A one-equation turbulence model for aerodynamic flows”. *La Recherche Aerospastiale*, Vol. 1, pp. 5–21.

Weisshaar, T.A., 2010. *Static and Dynamic Aeroelasticity. Encyclopedia of Aerospace Engineering*. John Wiley & Sons, New York, NY.

8. RESPONSIBILITY NOTICE

The authors are the only responsible for the printed material included in this paper.